

3-2012

## Response of a Carbonate Platform to the Cenomanian-Turonian Drowning and OAE 2: A Case Study from the Adriatic Platform (Dalmatia, Croatia)

Tvrtko Korbar  
*Croatian Geological Survey*

B. Glumac  
*Smith College, bglumac@smith.edu*

Blanka Cvetko Tesovic  
*University of Zagreb*

Sarah B. Cadieux  
*Mount Holyoke College*

Follow this and additional works at: [https://scholarworks.smith.edu/geo\\_facpubs](https://scholarworks.smith.edu/geo_facpubs)

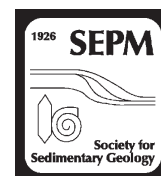


Part of the [Geology Commons](#)

### Recommended Citation

Korbar, Tvrtko; Glumac, B.; Tesovic, Blanka Cvetko; and Cadieux, Sarah B., "Response of a Carbonate Platform to the Cenomanian-Turonian Drowning and OAE 2: A Case Study from the Adriatic Platform (Dalmatia, Croatia)" (2012). Geosciences: Faculty Publications, Smith College, Northampton, MA. [https://scholarworks.smith.edu/geo\\_facpubs/164](https://scholarworks.smith.edu/geo_facpubs/164)

This Article has been accepted for inclusion in Geosciences: Faculty Publications by an authorized administrator of Smith ScholarWorks. For more information, please contact [scholarworks@smith.edu](mailto:scholarworks@smith.edu)



## RESPONSE OF A CARBONATE PLATFORM TO THE CENOMANIAN–TURONIAN DROWNING AND OAE 2: A CASE STUDY FROM THE ADRIATIC PLATFORM (DALMATIA, CROATIA)

TVRTKO KORBAR,<sup>1</sup> BOSILJKA GLUMAC,<sup>2</sup> BLANKA CVETKO TEŠOVIĆ,<sup>3</sup> AND SARAH B. CADIEUX<sup>4</sup>

<sup>1</sup>Croatian Geological Survey, Department of Geology, Zagreb, Croatia

<sup>2</sup>Department of Geosciences, Smith College, Northampton, Massachusetts, U.S.A.

<sup>3</sup>Department of Geology and Paleontology, Faculty of Science, University of Zagreb, Croatia

<sup>4</sup>Department of Geology, Mount Holyoke College, South Hadley, Massachusetts, U.S.A.

e-mail: tvrtko.korbar@hgi-cgs.hr

**ABSTRACT:** Global perturbations during the Cenomanian–Turonian boundary (CTB) interval and the Oceanic Anoxic Event 2 (OAE 2) represent one of the most extensively studied past environmental changes. To explore the response of various carbonate-platform depositional systems to such major environmental perturbations, strata of the intra-Tethyan Adriatic carbonate platform (*sensu stricto*) from the island of Brač (Adriatic Sea, Croatia) provide excellent exposures and a previously well-established Upper Cretaceous lithostratigraphic framework. Within this context, this study integrated lithostratigraphy, biostratigraphy, and chemostratigraphy to describe a drowned-platform succession underlain and overlain by peritidal carbonates. Carbon-isotope stratigraphy of this succession revealed a shift towards positive  $\delta^{13}\text{C}$  values that reached +4 to +5‰ VPDB, and represent the CTB interval excursion plateau.

We observed variations in thickness of the drowned-platform successions and explained them by three superimposed mechanisms: (1) diachronous drowning of platform relief; (2) intra-platform redeposition of parts of the successions by various mass-gravity transport processes (indicating enhanced instability due to increasing accommodation space related to the late Cenomanian platform drowning and syndimentary tectonics); and (3) migration of major carbonate factories during the recovery of shallow-platform environments. The results indicate that the CTB interval event caused unusual increase in accommodation space on the carbonate platform enabling open-marine influence and syndimentary redeposition. However, widespread organic-rich black shales reported from coeval strata of other regions have not been documented from the platform-top successions to date, and were probably accumulated in deeper (anoxic) settings below the rising sea level.

### INTRODUCTION

The geological time interval across the Cenomanian–Turonian boundary (CTB) records an important and well-studied global anoxic event—Oceanic Anoxic Event 2 (OAE 2). Numerous previous multifaceted examinations of this interval resulted in comprehensive datasets for subsequent comparative studies, especially those utilizing carbon-isotope stratigraphy (Arthur et al. 1987; Schlanger et al. 1987; Weissert 1989; Jenkyns et al. 1994; Davey and Jenkyns 1999; Kump and Arthur 1999; Jarvis et al. 2006; Pearce et al. 2009; among others). Consequently, a positive carbon-isotope excursion at the CTB is one of the best-documented examples of global carbon-cycle perturbations. Of particular interest for these studies is a response of various depositional systems to such major environmental perturbations.

The response of shallow marine settings to OAE 2 is still not well understood. Biostratigraphic records of shallow marine strata are generally poor and of rather low resolution, and, as a result, these environments have received relatively little attention to date (Gertsch et al. 2010; and references therein). This generalization is especially true for carbonate platform successions in which OAE 2-related records are difficult to recognize and document with certainty, and which consequently allow for multiple stratigraphic interpretations (e.g., Jenkyns 1991; Gušić and Jelaska 1993; Davey and Jenkyns 1999; Parente et al. 2007).

Carbon isotope chemostratigraphy can also be difficult to apply to shallow marine-platform carbonate deposits, because they are prone to alteration, especially during early diagenesis in the presence of meteoric fluids. In addition, oxidation of organic matter, photosynthesis, and biogenic respiration can result in  $\delta^{13}\text{C}$  values of semi-restricted water masses on carbonate platforms that are substantially different from those of the open ocean (Immenhauser et al. 2008; and references therein). Furthermore, carbonate shelves can have proximal-to-distal gradients in their carbon-isotope composition (Immenhauser et al. 2008; but also see Swart et al. (2009) for the lack of evidence for significant spatial variation and trends in  $\delta^{13}\text{C}$  composition of sediment on the present-day Great Bahama Bank), and are generally characterized by the highly complex interaction of sedimentological, physicochemical, and biological processes that affect the  $\delta^{13}\text{C}$  records (Immenhauser et al. 2008). All of these factors can hinder global correlation of shallow marine carbonate deposits.

Laminated black shale, the most characteristic OAE 2-related deposit, are normally absent from carbonate platform successions, making the recognition, interpretation, and correlation of coeval carbonate deposits even more challenging. Such absence of black shales also implies that anoxic and/or dysoxic conditions probably did not reach the uppermost water column during the OAE 2. However, considering the challenges and

uncertainties of the previous comparative studies of the CTB interval, several questions remain unresolved: Did low-oxygen water masses reach platform tops during the OAE 2 and, if so, what was their impact on platform biota? What was the temporal relationship between the CTB-interval sea-level rise, platform drowning, and the OAE 2? What was the overall carbonate platform response to the CTB environmental perturbations?

Our investigation of complete and well-exposed CTB intervals within carbonate platform successions provide some insights into these questions. The CTB interval of the intra-Tethyan Adriatic carbonate platform is characterized by a major facies change (Gušić and Jelaska 1993; Vlahović et al. 2005). This study focuses on integrating lithostratigraphy, biostratigraphy, and chemostratigraphic data from two coastal exposures through the Cenomanian–Turonian succession of the Adriatic carbonate platform (*sensu stricto*, Fig. 1), aimed at assessing impacts of the CTB interval and OAE 2 changes. New data include biostratigraphic analyses that improve and confirm age interpretations of the deposits in question and chemostratigraphic carbon-isotope analyses of carefully selected samples. This integrated case study provides detailed interpretation of responses of carbonate platforms to the combined influences of local tectonics and global oceanographic perturbations during the critical late Cenomanian and early Turonian time interval.

#### GEOLOGICAL SETTING

The present-day peri-Adriatic area (central-northern Mediterranean; Fig. 1A, B) represents the deformed sedimentary cover of the Adriatic microplate or Adria (Channell et al. 1979). During the Late Triassic to the Early Jurassic, several extensive and long-lived isolated carbonate platforms developed in the area (Zappaterra 1994; Vlahović et al. 2005; Korbar 2009; Fig. 1A). The largest among them was the Adriatic–Dinaridic carbonate platform (ADCP; cf. Jenkyns 1991; Gušić and Jelaska 1993; Pamić et al. 1998; Jelaska 2002), also named the Adriatic carbonate platform (AdCP; cf. Vlahović et al. 2005). This platform was a low-latitude, mainly shallow-marine system (Dercourt et al. 2000), comparable to the Bahama banks today. Its subsidence was balanced by prolific carbonate production, which is reflected in the deposition of a several-kilometer-thick carbonate succession during the Triassic to the Paleogene (Jelaska 2002). The Cenozoic tectonic evolution of the Mesozoic layer-cake platform carbonates was controlled by a series of Alpine orogenic events, forming a complex fold-and-thrust belt of the External Dinarides along the northeast margin of the Adriatic Sea (Pamić et al. 1998; Korbar 2009).

The best exposures of Upper Cretaceous strata of the Adriatic carbonate platform succession (Fig. 1A) are on the island of Brač in the central Dalmatian region of Croatia (Fig. 1B, C). The CTB interval is recorded within this typical central-Tethyan carbonate platform, and excellent coastal outcrops on Brač (Fig. 1D) allow a unique opportunity to study this important stratigraphic interval in great detail.

Carbonate deposits exposed along the western coast of Brač (Fig. 1D) belong to the Milna, Sveti Duh, and Gornji Humac formations (Gušić and Jelaska 1990). The Milna Formation, of Cenomanian age, represents the oldest deposits on Brač. Carbonate facies in this formation include a variety of skeletal lithofacies (including rudists, other mollusks, and foraminifera) with common microbial lamination, occasional slump features, and rare intraformational breccia. Similar to the Milna Formation laminites, Cenomanian fish-bearing carbon-rich platy limestones (Komen Limestone) present elsewhere in the region have been interpreted previously to represent deposition during the expansion of the oxygen-minimum zone from the surrounding basins onto the platform top during the CTB event (Jenkyns 1991). However, these fish-bearing limestones were deposited prior to the CTB event (Gušić and Jelaska 1993; Korbar et al. 2001; Palci et al. 2008). The Milna Formation is overlain by the Sveti Duh Formation, which is dominated by micritic

limestones with pelagic microfossils such as calcispheres and planktonic foraminifera. The lowermost part of the overlying Gornji Humac Formation is composed of thick-bedded micritic limestone and packages of packstone–grainstone with angular mollusk bioclasts.

The transition between the Milna and Sveti Duh formations is a major lithological change within the CTB interval succession. This change has been interpreted to represent an overall sea-level rise that caused pelagic sedimentation on top of the platform (Gušić and Jelaska 1990, 1993). Based on limited fossil evidence, Gušić and Jelaska (1990) placed the CTB at the contact of the Milna and Sveti Duh formations. However, chronostratigraphically diagnostic or characteristic index fossils have not been identified in the Sveti Duh Formation, making a more precise age determination of these deposits difficult. According to Gušić and Jelaska (1990), these strata are most likely early Turonian, although the lowermost Sveti Duh may be late Cenomanian.

#### MATERIALS AND METHODS

Two carbonate rock successions on the western coast of Brač (Fig. 1) were measured, sampled, and described. The Brač–Bobovišća–Kupinova succession (BBK, Fig. 2), is 84.5 m thick and located at the Kupinova cove on the SW coast of the Bobovišća Bay (Fig. 1D). In total, 89 micritic samples were collected from this succession for carbon and oxygen isotope analyses. The Brač–Splitska Vrata (BSV) succession is 110 m thick (Fig. 3), and is located at the westernmost coast of the island, about 4 km SW of BBK (Fig. 1D). Samples for isotopic analyses were collected at approximately 1 m intervals for a total of 114 samples. Selected samples (43 from BBK and 28 from BSV) were examined for micropaleontology.

Small amounts (2–3 mg) of powder for isotopic analyses were obtained from polished slabs and thin-section billets, using a microscope-mounted microdrill. To produce a reliable, high-resolution isotopic curve, we attempted to carefully select and drill only the material that was micritic, homogeneous, monomineralic, and non-weathered. Although aimed at excluding areas with carbonate cement and skeletal fragments, it was especially challenging to drill pure micrite from wackestone and packstone deposits. Therefore, material from small bioclasts (e.g., echinoderms, foraminifera, mollusks) may be present in samples from such deposits. Stable-isotope analyses were performed at the University of Massachusetts-Amherst using a Kiel III on-line automated carbonate preparation system coupled directly to Finnegan-MAT DeltaXL + mass spectrometer. After heating for an hour at 400°C to remove any volatile organic components, samples were reacted at 70°C with 100% anhydrous phosphoric acid (H<sub>3</sub>PO<sub>4</sub>) for ten minutes. Standard isobaric and phosphoric acid fractionation corrections were applied to all data. Internal analytical precision, monitored through daily analysis of carbonate standards, was better than or equal to 0.1‰ for both carbon and oxygen isotope values. Stable-isotope results are expressed as δ<sup>13</sup>C and δ<sup>18</sup>O values in ‰ relative to the Vienna PeeDee Belemnite standard (VPDB).

Curves connecting five-point running-average values for both carbon and oxygen isotope data were constructed and compared to stratigraphic columns of the two successions. A comparison of δ<sup>13</sup>C and δ<sup>18</sup>O data evaluated the presence of diagenetic modification and the carbon-isotope curves were compared to the reference curves for this interval (Davey and Jenkyns 1999; Gale et al. 2005; Pearce et al. 2009) and used to improve stratigraphic interpretations of these deposits and for their local to global correlation.

#### RESULTS

##### *Lithostratigraphy*

**Brač–Bobovišća–Kupinova (BBK) Locality (Figs. 2, 4A).**—The basal portion of BBK, designated as the Milna Formation, is represented by

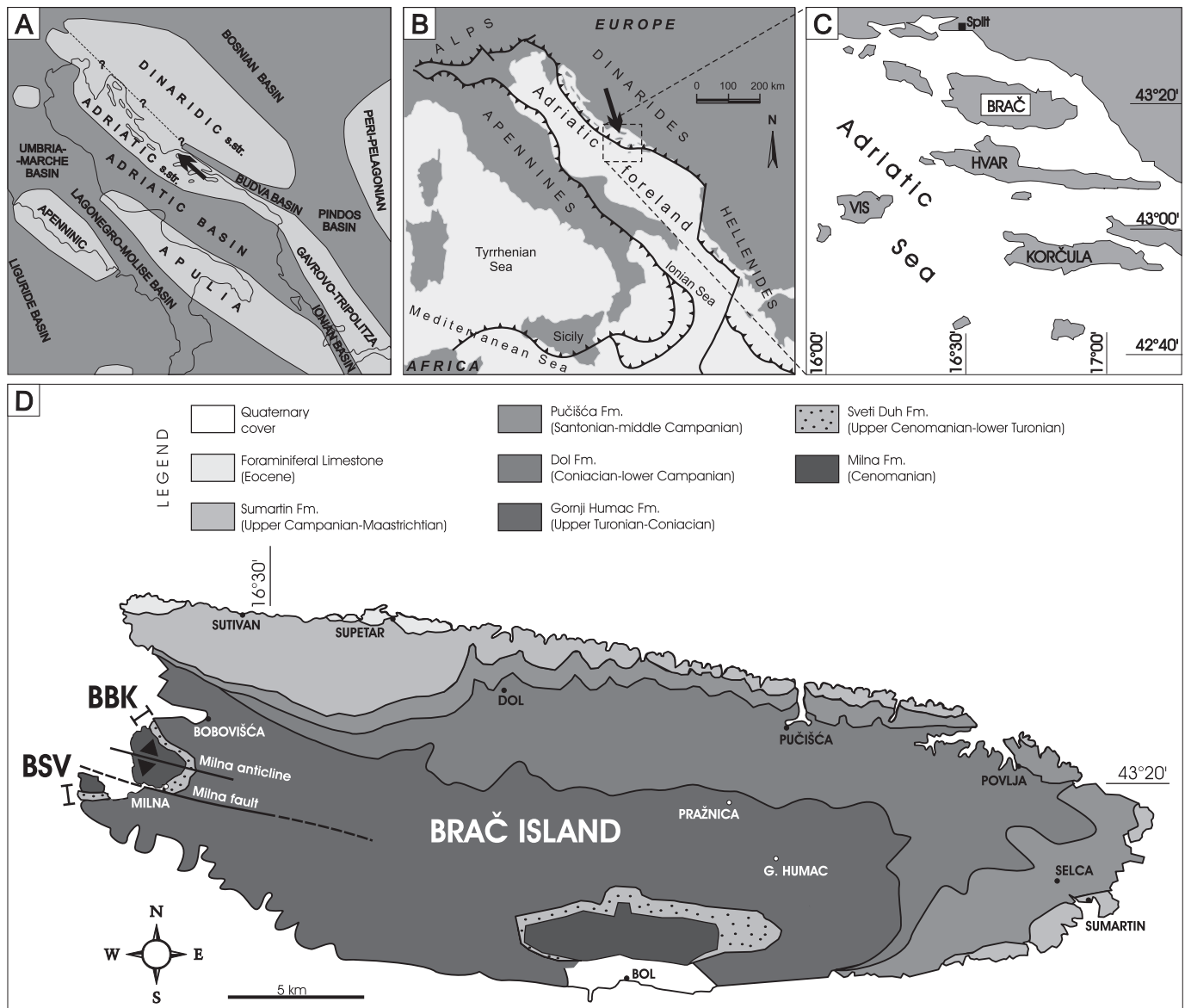


Fig. 1.—Study area. **A**) Paleogeographic map of the Late Cretaceous (platforms and shelves = light gray, basins and oceans = dark grey; modified after Korbar 2009), and location of the island of Brač (arrow). **B**) Regional tectonic map and location of Brač (arrow) (modified after Korbar 2009). **C**) Geographic location of Brač in central Dalmatia (Croatia). **D**) Simplified geological map of Brač (modified after Gušić and Jelaska 1990, and Steuber et al. 2005), and position of the investigated sections (BSV and BBK).

30.5 m of peritidal limestones and intraformational carbonate breccias (Fig. 4B–F). The lowermost interval (0.0–8.0 m) is characterized by thick-bedded skeletal–bioclastic limestone containing abundant benthic foraminifera, gastropods, peloids, and rare ostracod fragments (commonly forming foraminiferal grainstone), as well as chondrodontid bivalve lithosomes with thin-shelled radiolitid rudists. Dissolutional and intra-skeletal voids commonly are filled with clear equant calcite cement (Fig. 5A). Neptunian dikes, infilled with bioclastic wackestone to packstone containing calcispheres, calcispheric wackestone–packstone intraclasts, and lithoclasts of laminated limestones (Fig. 5B), cut strata normal to bedding. A deformed laminated mudstone interval with single-fold slumps (Fig. 4B) is present from 8 m to 15.7 m. These deposits have typical microbial wavy laminae and also contain fenestrae, peloids, rare foraminifera (characteristic of brackish environments; Fig. 5C, D), and pockets of intraclasts and pseudoclasts. On top of the laminated interval

(at 15.7 m), meter- to decameter-scale blocks of bioclastic–skeletal packstone, grainstone, and floatstone (similar to the lowermost interval of the BBK succession) are in a sharp, sliding contact with the underlying laminites (Fig. 4C). Unsorted carbonate breccia (Fig. 4D) is irregularly interbedded within the deformed laminites (Fig. 4E), forming irregular meter-scale pockets and lenticular bodies. The breccias contain centimeter- to decimeter-scale angular light-gray intraclasts of micritic and bioclastic peritidal limestones, radiolitid–rudist bioclasts, as well as dark-grey or brownish intraclasts of calcispheric-microbioclastic wackestone–packstone.

Directly overlying the Milna Formation with a sharp contact at 30.5 m (Fig. 4F) is a 41-m-thick succession designated as the Sveti Duh Formation. The first bed of the Sveti Duh Formation, which directly overlies the uneven upper surface of the folded Milna Formation laminites, is characterized by normally graded bioclastic wackestone–packstone with



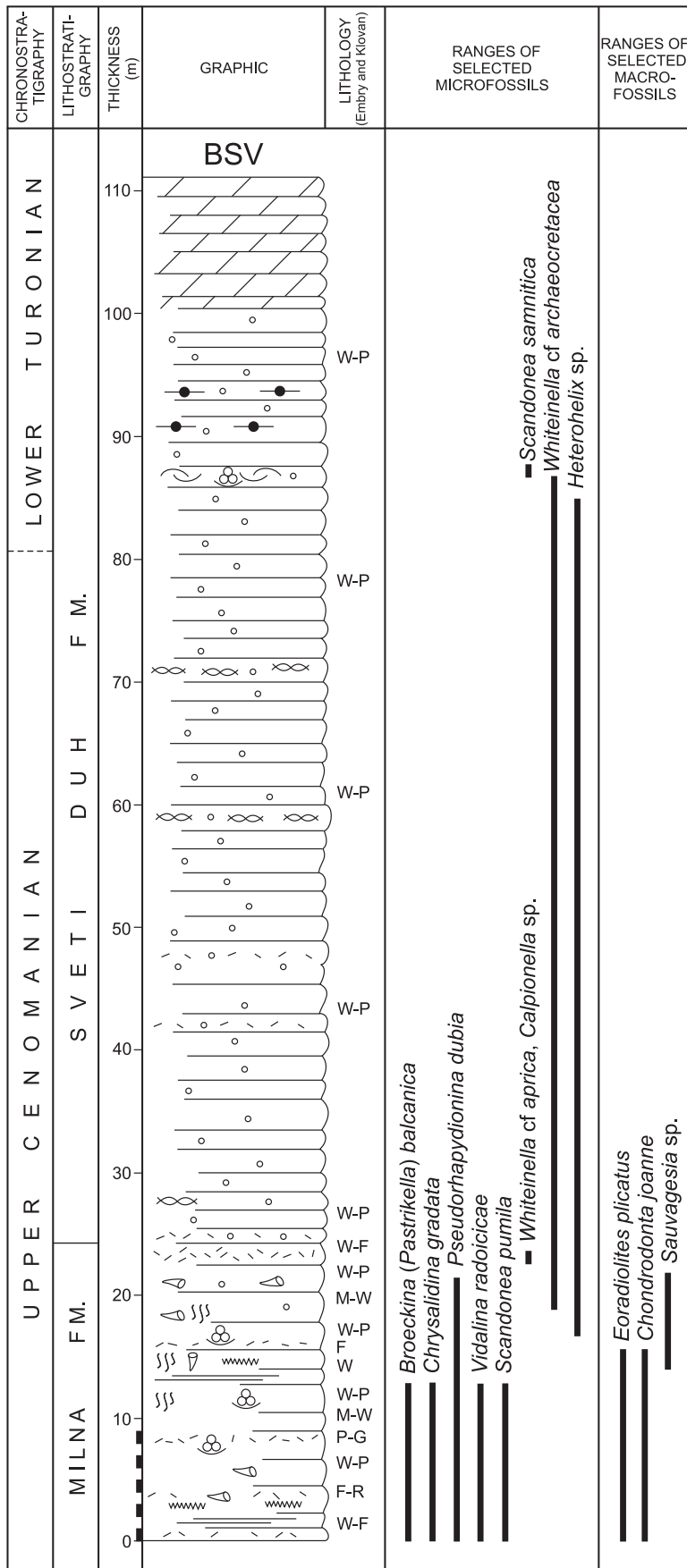


FIG. 3.—Stratigraphic column of the BSV succession (for legend see Fig. 2).



benthic foraminifera and calcispheres. Overlying beds are composed predominantly of calcispheric wackestone–packstone with microbioclasts and planktonic foraminifera (Fig. 5E), millimeter-scale echinoderm and sponge fragments, ostracodes, gastropods, thin-shelled bivalves, and rare weathered glauconitic grains. Very rare benthic foraminifera occur in the lower part of the succession (Fig. 5F). Rare oncoids exist in the middle part, which is in places bioturbated by *Thalassinoides*-type burrows (1–2 cm in diameter). The upper part of the Sveti Duh Formation at BBK is characterized by a few meter-thick package of bioclastic (angular, mainly mollusk), packstone–grainstone to floatstone–rudstone overlain by nodular calcispheric wackestone (Fig. 5K).

Approximately 15 m of the Gornji Humac Formation overlies the Sveti Duh Formation at the BBK locality. The lower part of the Gornji Humac Formation is composed of thick-bedded mudstone–wackestone with rare benthic foraminifera, algae, gastropods, and thick-shelled radiolitic rudists in growth position. The uppermost part of the succession is characterized by a few-meter-thick bioclastic packstone–grainstone to rudstone composed of angular, mainly mollusk clasts, organized in indistinct high-angle cross-beds.

**Brač–Splitska Vrata (BSV) Locality (Fig. 3).**—The basal portion of the BSV stratigraphic section is a 24.2-m-thick succession of peritidal limestones of the Milna Formation. These deposits represent interbedded bioclastic mudstone, wackestone, packstone, grainstone, and floatstone with chondrodontid bivalves, abundant benthic foraminifera, peloidal grains, common echinoderm fragments, and rare ostracods, as well as groups of thick-shelled radiolitic rudists, toppled and in life position. Mottling and bioturbation are common in these deposits. Rare laminations, dolomitization, and weathered pyrite are also present, particularly in the lower part of the Milna Formation outcrop. Thin intercalations of calcispheric wackestone containing planktonic foraminifera occur in the uppermost part of the succession (Fig. 5G, I, J).

Overlying the Milna Formation with a sharp, planar contact is an 85.8-m-thick succession of the Sveti Duh Formation, which is characterized by calcispheric wackestone to packstone containing planktonic foraminifera, echinoderm fragments, sponge spicules, and rare *Saccocoma* sp. (Fig. 5H). These rocks rarely contain macroscopic echinoderm bioclasts. At 42.1 m and 47.4 m of the BSV section, thin intercalations of microbioclastic–peloidal wackestone–packstone, with mollusk fragments and rare benthic biota (poorly preserved foraminifera and algae), are interbedded within the calcispheric wackestone–packstone. Nodular beds are present in the middle of the section, between 55 and 75 m stratigraphically, and chert nodules are between 90 and 95 m. An intercalation of thin-shelled bivalve floatstone with rare benthic foraminifera occurs at 87.6 m. The uppermost Sveti Duh Formation, from 100 m stratigraphically to the top of the section, is almost completely dolomitized, and its primary fabric commonly is obliterated.

### Biostratigraphy

Biostratigraphic analysis revealed the following late Cenomanian foraminiferal association in the Milna and the lowermost Sveti Duh formations (Fig. 5): *Vidalina radoicicae* (Fig. 5F), *Broeckina (Pastrickella) balcanica*, *Pseudohapydionina dubia*, *Chrysalidina gradata*, *Biplanta*

*peneropliformis*, *Cuneolina pavonia*, *Triloculina* sp., *Biconcava bentori*, *Rumanoloculina* sp., *Nezzazatinella* sp., *Nezzazata simplex*, *Axiopolina* sp., *Nezzazatinella picardi*, and *Spiroloculina* sp. In addition, Cenomanian rudist *Eoradiolites plicatus*, as well as chondrodontid bivalves *Chondrodonta joanne* and *Chondrodonta* cf. *glabra*, are also present in this interval.

In the BBK section, the late Cenomanian index fossils (*Pseudohapydionina dubia* and *Vidalina radoicicae*) occur in the drowned platform succession of the Sveti Duh Formation, 5 m above the boundary with the underlying Milna Formation (Fig. 2). The uppermost part of the Milna and the Sveti Duh formations also yielded planktonic foraminifera *Whiteinella* cf. *baltica* (Fig. 5E), *Whiteinella* cf. *archaeocretacea* (Fig. 5I), and *Whiteinella* cf. *aprica* (Fig. 5J), which are biostratigraphically significant index fossils of the CTB interval biozone. Characteristic Turonian foraminifera *Scandonea samnitica* (Fig. 5L) and *Moncharmontia* cf. *compressa* (Fig. 5M) are present in the uppermost part of the successions (Figs. 2, 3).

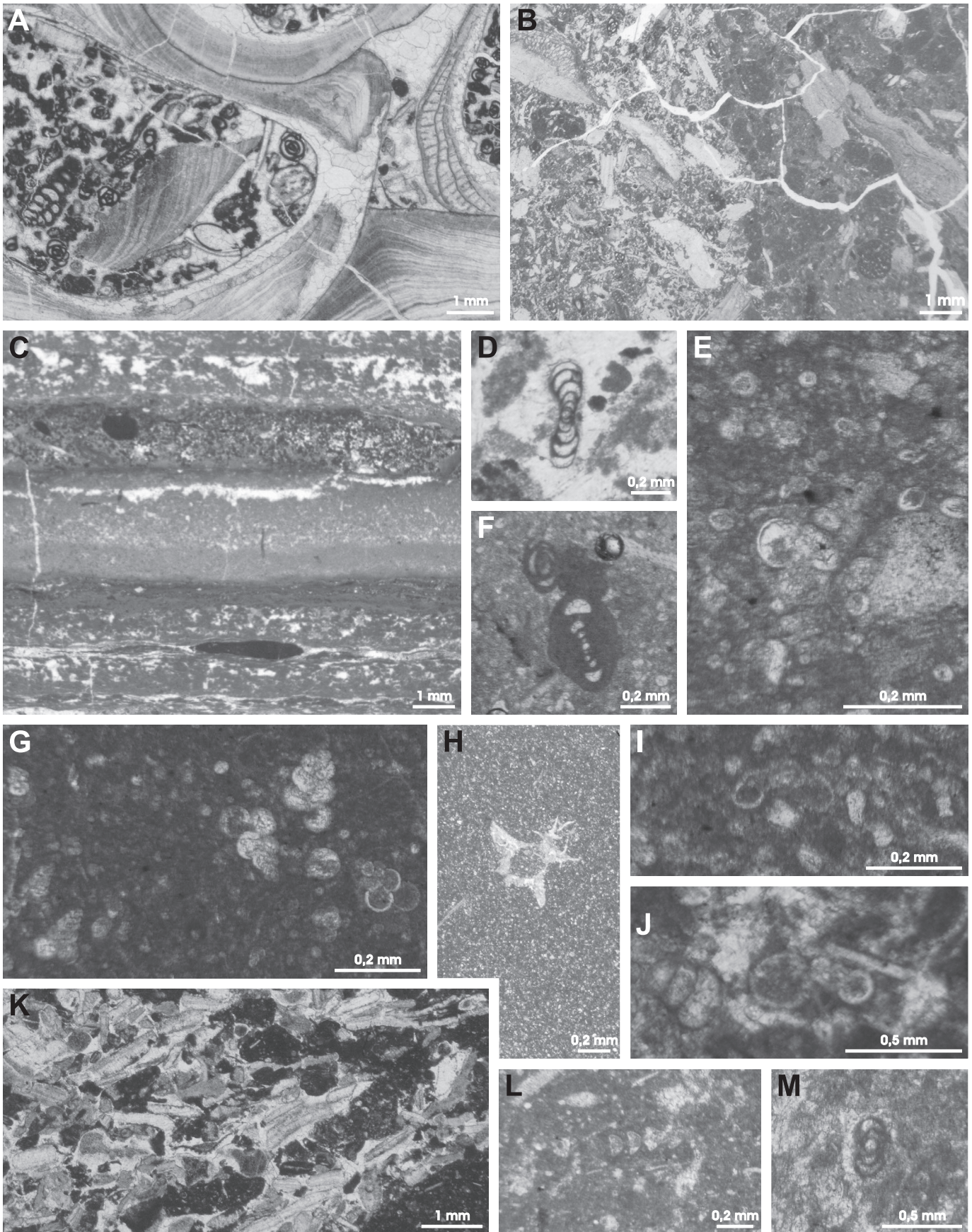
### Chemostratigraphy

**Carbon Isotopes of the Brač–Bobovišća–Kupinova (BBK) Locality.**—A wide range of  $\delta^{13}\text{C}$  values is observed in the Milna Formation, from  $-5.8\text{‰}$  (at 14.5 m) to  $+1.8\text{‰}$  (at 28.1 m), at BBK (Fig. 6). The data scatter increases in the uppermost part of the formation and, consequently, the carbon-isotope curve is not as clearly defined in this part of the succession as in the lower Milna Formation. Little change in  $\delta^{13}\text{C}$  values is present directly above or below the Milna–Sveti Duh formational boundary. In the lowermost Sveti Duh Formation, the  $\delta^{13}\text{C}$  values are about  $+2\text{‰}$ . Less than 5 m above the contact between the Milna and the Sveti Duh formations, at 34.6 m, the carbon-isotope values increase from  $+2.2$  to  $+5.0\text{‰}$ . From 36.6 m up to 55.4 m of stratigraphic thickness, the values remain positive, mainly around  $+4\text{‰}$  and up to  $+6\text{‰}$ . Upsection, from 55.4 m to the top of section, there is more data scatter ( $\delta^{13}\text{C}$  values range from  $+1.7$  to  $+6.1\text{‰}$ ) and the carbon-isotope curve is not clearly defined (Fig. 6).

**Carbon Isotopes of the Brač–Splitska Vrata (BSV) Locality.**—In the Milna Formation at BSV, the  $\delta^{13}\text{C}$  values generally range from  $-1$  to  $+3\text{‰}$  (Fig. 6). The carbon-isotope curve is fairly well defined, with individual values fluctuating more in the lower than upper part of the formation. The Milna–Sveti Duh boundary interval is marked by generally high  $\delta^{13}\text{C}$  values (reaching up to  $+3.6\text{‰}$ ) and defining a positive peak on the carbon-isotope curve (labeled as peak “a” between about 20 and 25 m above the base of the section, Fig. 6). In the lower part of the Sveti Duh Formation (up to about 52 m stratigraphically), a large fluctuation in the  $\delta^{13}\text{C}$  values is evident. This part of the section contains both the minimum and maximum values of the entire succession:  $-4.7\text{‰}$  (at 32.9 m) and  $+5.4\text{‰}$  (at 44.5 m; Fig. 6). Due to this large scatter, this part of the carbon-isotope curve is not clearly defined, although it exhibits a positive peak between about 40 and 47 m stratigraphically (labeled as peak “b” on Fig. 6). The rest of the Sveti Duh Formation ( $\sim 52$  m to the top of section) has positive  $\delta^{13}\text{C}$  values, ranging from  $+1.1$  to  $+4.4\text{‰}$ . A well-defined carbon-isotope curve, with  $\delta^{13}\text{C}$  values averaging  $+3.5\text{‰}$ , continues up to about 100 m of stratigraphic thickness, with a possible small positive peak (indicated as peak “c” on Fig. 6) marked by the  $\delta^{13}\text{C}$

←

Fig. 4.—Field photographs of the BBK succession. **A**) Exposure at the eastern coast of Kupinova cove (bedding planes of the key horizons are marked). **B**) Laminated and platy limestones of the Milna Formation and a single-fold slump of southern vergence (arrow). **C**) Sharp contact of the Milna laminites below and a slide block of skeletal–peloidal packstone above. **D**) Carbonate breccia of the disturbed upper part of the Milna Formation. **E**) Chaotic slump in the uppermost disturbed part of the Milna Formation. **F**) Sharp contact of the underlying chaotically folded laminite (chaotic slump) of the Milna Formation and the overlying calcispheric–microbioclastic wackestone–packstone of the Sveti Duh Formation.



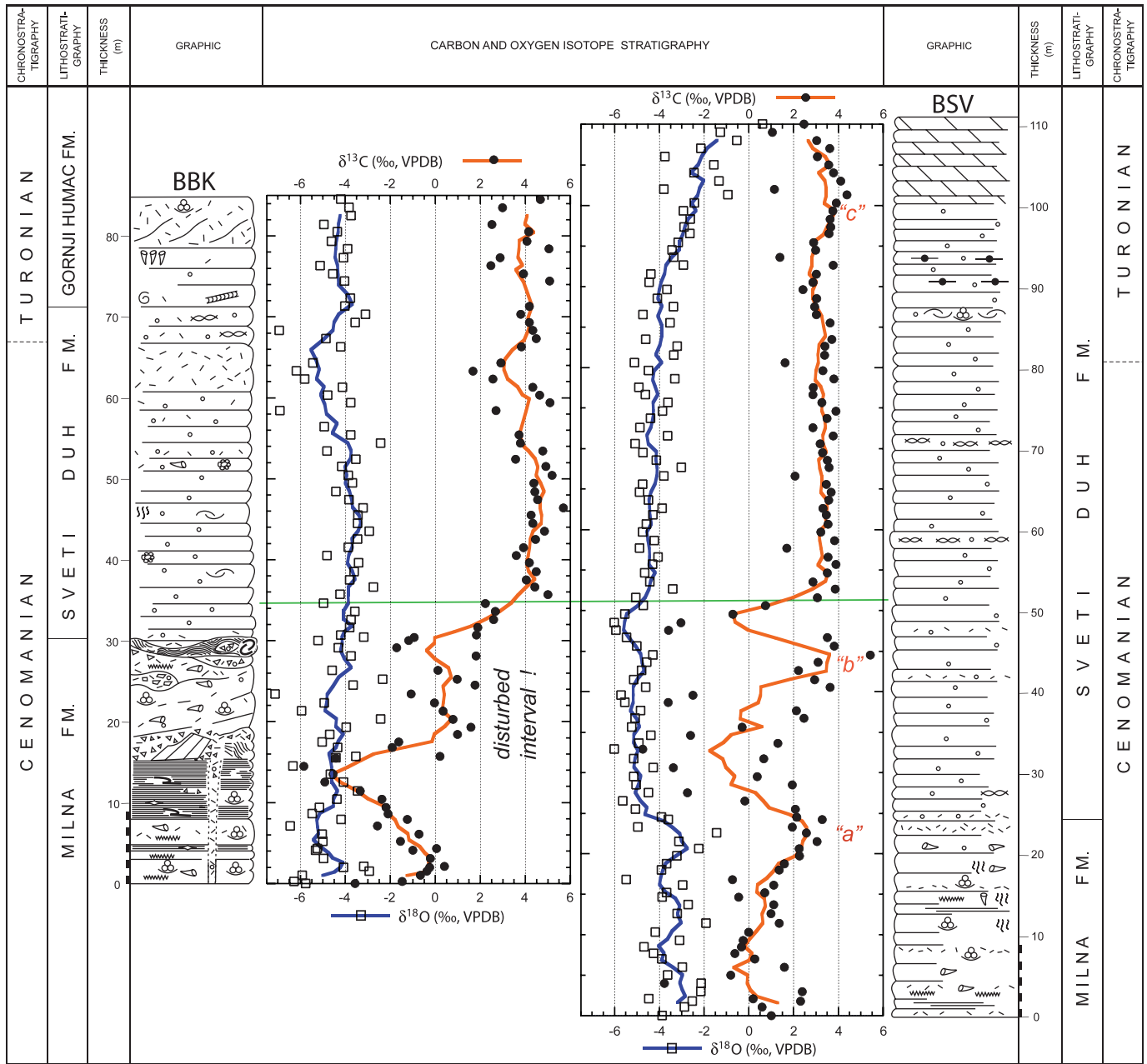


FIG. 6.—Carbon-isotope ( $\delta^{13}\text{C}$ ) correlation of the BBK and BSV successions from the western part of the island of Brač with tentative interpretation of *a*, *b*, and *c* peaks of the  $\delta^{13}\text{C}$  curve for the Eastbourne reference Cenomanian–Turonian Boundary (CTB) section (after Pearce et al. 2009). Correlation line is placed at the beginning of the CTB excursion plateau.

←

FIG. 5.—Photomicrographs of the microfacies and index fossils. **A**) Washed rudstone of the Cenomanian chondrodontid–rudist (*Eoradiolites plicatus*) facies of the Milna Formation from 2.0 m of the BBK section. **B**) Bioclastic–skeletal packstone–grainstone of the Milna Formation (on the left) and neptunian dike (on the right) with calcispheric–microbioclastic wackestone–packstone, intraclasts, and, lithoclasts of laminite from 1.5 m of the BBK section. **C**) Laminite with foraminifera characteristic of brackish conditions from 12.5 m of BBK section. **D**) *Spirolina* sp. from 12.5 m of the BBK section. **E**) Typical calcisphere wackestone of the Sveti Duh Formation with *Whiteinella* cf. *baltica* from 39.7 m of the BBK section. **F**) Late Cenomanian index microfossil *Vidalina radoicicae* from 35.7 m of the BBK section. **G**) Bioclastic wackestone with different sections of *Heterohelix* sp. cf. *H. reussi* from 75.0 m of the BSV section. **H**) Bioclastic wackestone with *Saccocoma* sp. from 26.05 m of the BSV section. **I**) *Whiteinella* cf. *archaeoeretacea* from 18.75 m of the BSV section. **J**) *Whiteinella* cf. *aprica* from 22.55 m of the BSV section. **K**) Bio–lithoclastic packstone–grainstone and floatstone–rudstone with predominantly echinoderm fragments inserted in pelagic matrix (bioclastic wackestone) from 62.2 m of the BBK section. **L**) *Scandonea samnitica* from 87.6 m of the BSV section. **M**) *Moncharmontia* cf. *compressa* from 84.4 m of the BBK section.

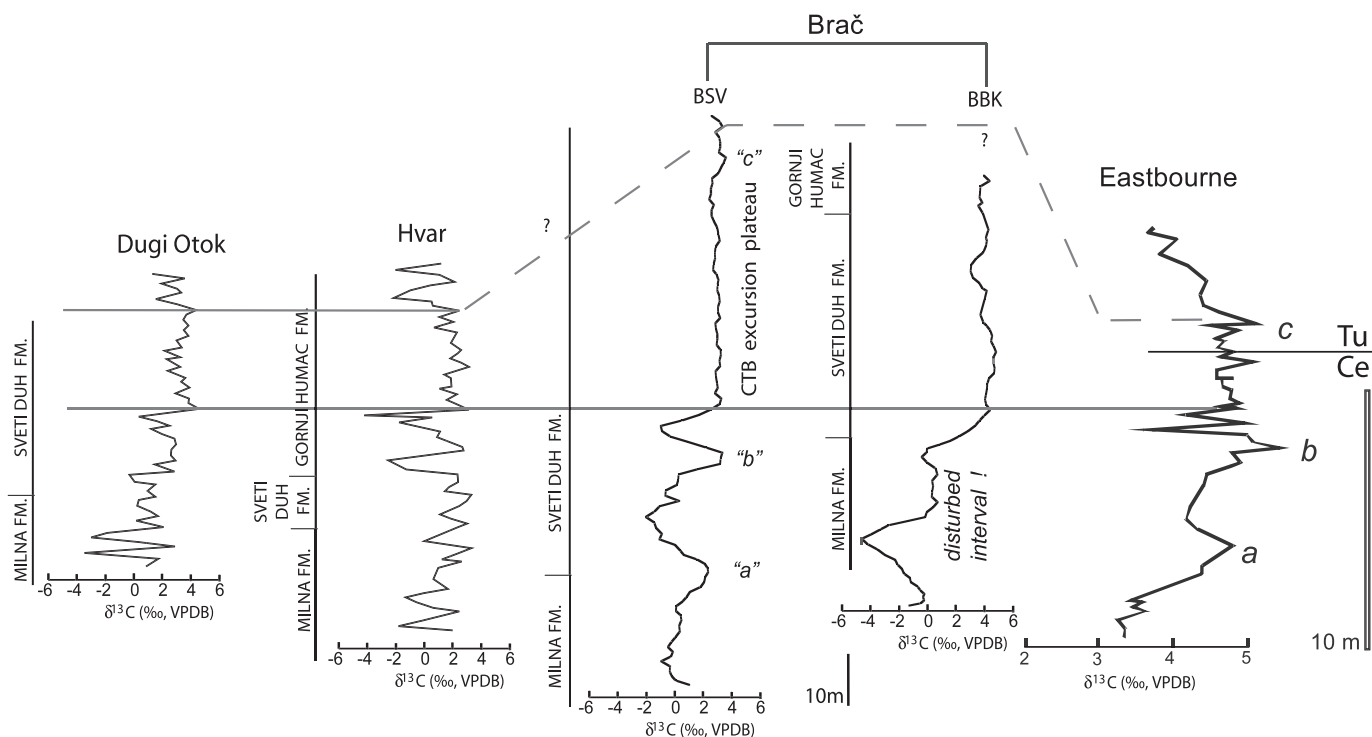


FIG. 7.—Carbon-isotope ( $\delta^{13}\text{C}$ ) correlation of the CTB interval regionally (Dugi Otok and Hvar data after Davey and Jenkyns 1999) and globally (the Eastbourne reference section). Letters *a*, *b*, and *c* mark the characteristic peaks of Pearce et al. (2009).

values greater than +4‰ in the stratigraphic interval between 100 and 103 m. In the uppermost 10 m of the section, which is dolomitic, a well-defined curve is maintained, exhibiting a trend of decreasing  $\delta^{13}\text{C}$  values from +4.4‰ to +2.5‰ upsection.

**Oxygen Isotopes.**—For both BBK and BSV, all  $\delta^{18}\text{O}$  values fall between +0.5 and  $-7\text{‰}$  (Fig. 6). At BSV, the Milna Formation includes similar trends in carbon and oxygen-isotope curves, both decreasing up to 7 m stratigraphically, and then increasing upsection to the top of the Milna Formation, with  $\delta^{18}\text{O}$  values centering around  $-4\text{‰}$  (Fig. 6). In the lower Sveti Duh Formation at BSV,  $\delta^{18}\text{O}$  values decrease slightly and primarily remain centered around  $-5\text{‰}$ , which is in contrast to the highly variable  $\delta^{13}\text{C}$  values of this part of the succession. A negative peak occurs in both carbon- and oxygen-isotope curves at about 50 m stratigraphically (Fig. 6). Above this peak, the  $\delta^{18}\text{O}$  values gradually increase from  $-5$  to  $-4\text{‰}$ , corresponding to the relatively uniform  $\delta^{13}\text{C}$  values. The decrease in the  $\delta^{13}\text{C}$  values in the uppermost part of the BSV succession coincides with a trend of increasing  $\delta^{18}\text{O}$  values (Fig. 6).

At BBK, the large variations in  $\delta^{13}\text{C}$  are generally not matched by  $\delta^{18}\text{O}$  values. However, some covariant trends can be observed in isotope curves in parts of the successions (i.e., the lowermost part of the Milna and the uppermost part of the Sveti Duh Formation; Fig. 6). In the lower part of the Sveti Duh Formation, the large scatter in  $\delta^{13}\text{C}$  values corresponds to a much smaller scatter in  $\delta^{18}\text{O}$  values (mainly between  $-6$  and  $-4\text{‰}$ ). In the upper section of the Sveti Duh and the overlying Gornji Humac formations, both  $\delta^{18}\text{O}$  and  $\delta^{13}\text{C}$  values remain relatively uniform and yield well-defined curves with only a small negative peak at about 65 m stratigraphically (Fig. 6).

## INTERPRETATIONS AND DISCUSSION

### Carbon-Isotope Stratigraphy

Large scatters in isotope data from the lower part of both BSV and BBK successions are likely related to diagenetic modification of micritic

matrix but could also in part represent sample contamination from small bioclasts. The relatively negative  $\delta^{13}\text{C}$  values (reaching almost  $-6\text{‰}$ ) documented for the Milna and lower part of the Sveti Duh formations at BSV and the Milna Formation of BBK most likely reflect alteration by meteoric fluids. Similarly,  $\delta^{18}\text{O}$  values from both BBK and BSV localities range from +1 to  $-7\text{‰}$  and suggest alteration of original marine  $\delta^{18}\text{O}$  values in most samples (Fig. 6). Diagenetic modifications are also indicated by the covariance between carbon- and oxygen-isotope values observed in some parts of the successions (Fig. 6). Although detailed diagenetic analysis was beyond the scope of this study, in both BBK and BSV, recrystallization of micrite as well as dissolution and precipitation of clear calcite cement constitute evidence for early meteoric diagenesis. Similarly, Davey and Jenkyns (1999) invoked minor meteoric diagenetic alteration in interpreting carbon-isotope variations in the coeval successions from the central Adriatic region of Croatia (Hvar and Dugi Otok islands; Fig. 7).

Carbon-isotope curves for the upper parts of BBK and BSV successions are generally better defined with more uniform and less scattered values (Fig. 6). Deposits from these parts of the successions have likely experienced no major systematic resetting of  $\delta^{13}\text{C}$  values during diagenesis, and they reveal important trends in secular carbon-isotope variations. Carbon-isotope values of these deposits are generally more positive and cluster between +1 to +6‰ (Fig. 6). Similar studies documenting the CTB interval have observed carbon-isotope ranges from +1 to +5.5‰ (Jarvis et al. 2006; Parente et al. 2007), associated with a well-documented secular positive carbon-isotope excursion. Elsewhere, the carbon-isotope record of the CTB interval has been related to chronostratigraphy using both index fossils and ash beds (Paul et al. 1999; Desmares et al. 2007). This allows the patterns of completely documented CTB positive carbon-isotope excursion from locations without adequate biostratigraphy or datable ash beds, such as Brač, to be divided into several intervals and correlated with stratigraphically well-defined profiles elsewhere. The Eastbourne profile (Jarvis et al. 2006; and references

therein), from Eastbourne Gun Gardens, England, is the most detailed isotopic record of the CTB event, recording the pre-excursion, the first build up (or peak *a*, cf. Pearce et al. 2009), the trough, the second build-up (peak *b*, cf. Pearce et al. 2009), the plateau (ending with peak *c*, cf. Pearce et al. 2009), and recovery of the  $\delta^{13}\text{C}$  values to the pre-excursion levels. In the Eastbourne succession, the base of the Turonian is marked biostratigraphically by the appearance of the ammonite *Watinoceras* and the bivalve *Mytiloides puebloensis*, placing the CTB near the end of the excursion plateau. Similar Cenomanian–Turonian excursion plateaus were observed on the Crimean Peninsula, in Ukraine (Fisher et al. 2005), in the Western Interior Basin, USA (Desmares et al. 2007), and in black shales of Port d'Issole, France (Grosheny et al. 2006).

When compared to the Eastbourne carbon-isotope reference curve (Jarvis et al. 2006; Pearce et al. 2009) the CTB excursion plateau is observed in both BSV and BBK (Fig. 7). The three major excursion peaks (*a*, *b*, and *c*; cf. Pearce et al. 2009) are only tentatively recognized in the more complete and undisturbed BSV profile due to the uncertainties related to scattered carbon-isotope values from diagenetic overprinting. The first peak “*a*” marks the onset of the Plenian Cold Event, while the second peak “*b*” directly precedes one of the most severe intra-Cretaceous biotic crisis during the latest Cenomanian (Pearce et al. 2009). The uniformly positive, averaging +3.5‰, carbon-isotope values of the Sveti Duh Formation in both successions represent the CTB excursion plateau (above the correlation line in Figs. 6 and 7). Above the possible third peak (tentative peak “*c*” with  $\delta^{13}\text{C}$  values > 4‰) in the upper part of the BSV succession, the trend of decreasing values upsection (from +4 to +2‰) hints at the end of the CTB interval event (Fig. 6).

At BBK, the carbon-isotope curve is not as well defined as in BSV, since the succession is partly disturbed (redeposited). As in BSV, the start of the CTB plateau is placed within the Sveti Duh Formation, at approximately 35 m above the base of section where the  $\delta^{13}\text{C}$  value jumps from +2.2‰ to +5.0‰ (Figs. 6, 7). Along the plateau to the top of the succession, all carbon-isotope values are positive and above +2‰, with most ranging between +4 to +6‰. Unlike BSV, no trend in decreasing  $\delta^{13}\text{C}$  values upsection was observed at BBK (Fig. 6). Therefore, the top of the section is probably still within the CTB event. Even though the CTB plateau is present in the Sveti Duh Formation at both sections, 25 m of the Sveti Duh Formation were deposited prior to the beginning of the plateau in BSV, as compared to only 5 m in BBK (Figs. 6, 7). This indicates that although relatively close to each other, these two successions represent different depositional areas of the carbonate platform characterized by different sedimentation patterns.

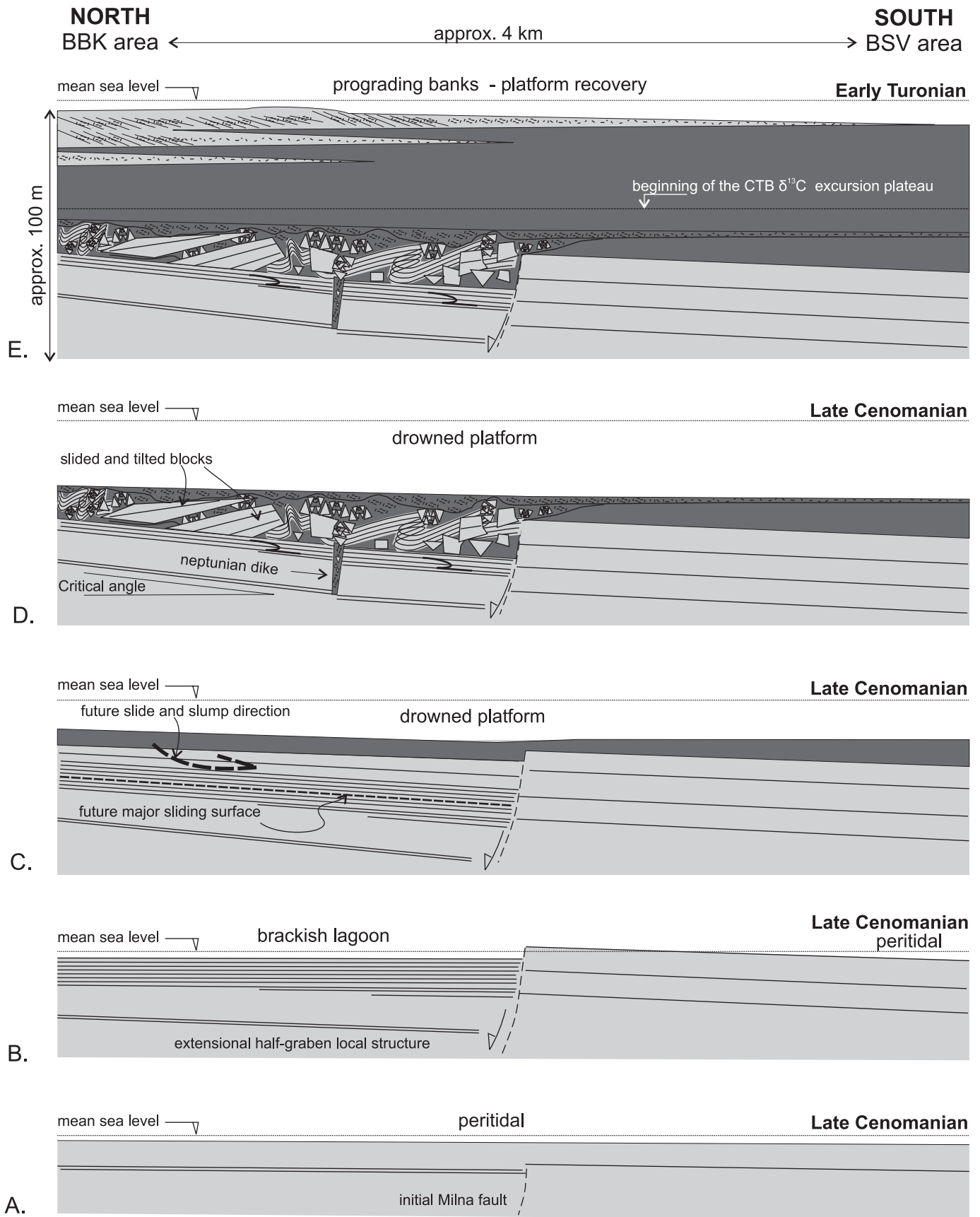
The CTB excursion plateau observed in the  $\delta^{13}\text{C}$  profiles from Brač can also be correlated with carbon-isotope records from carbonate platform successions elsewhere in the region, such as those of Davey and Jenkyns (1999), who examined two carbonate successions on the islands of Dugi Otok (approximately 120 km NW of Brač) and Hvar (approximately 20 km south of Brač) (Figs. 1, 7). At all of these localities, evidence for increased pelagic influence was observed during the CTB interval in the transition from restricted-platform deposition of the Milna Formation, to more open-marine deposits of the Sveti Duh Formation. The age and duration of the pelagic influence represented by the Sveti Duh Formation, however, vary between the localities: it occurs in the latest Cenomanian on Hvar, and across the CTB on Dugi Otok. Davey and Jenkyns (1999) defined the CTB event by a plateau of  $\delta^{13}\text{C}$  values greater than +3‰ (Fig. 7) with a number of inflection points that match the Eastbourne reference curve. The CTB plateau in the Hvar succession, however, is not clearly expressed, and different interpretations than those of Davey and Jenkyns (1999) are possible. Despite the difference in the type of carbon-isotope curves shown (five-point running average for BSV and BBK; line connecting all data points in Hvar and Dugi Otok), some similarities, such as the peaks before and after the excursion plateau, can be observed in Dugi Otok, Hvar, and BSV, and used for their correlation (Fig. 7).

Comparison with the carbon-isotope reference curves suggests that in BSV the CTB is within the upper part of the excursion plateau (Fig. 7). The placement of the boundary is difficult in the less complete BBK succession. The documented distribution of the late Cenomanian fossils in the Milna and the lowermost Sveti Duh deposits, and the results of carbon-isotope stratigraphy, suggest that the lowermost possible placement of the CTB is in the upper part of the excursion plateau. This placement is higher than previously proposed by Gušić and Jelaska (1990), and is in general agreement with the placement of the boundary in the middle of the pelagic succession on the island of Dugi Otok (Davey and Jenkyns 1999; Fig. 7). The observed differences in both stratigraphic thickness and lithostratigraphic characteristics of the deposits from the CTB interval in these successions reflect details in sediment accumulation records across the platform related to its differentiation due to synsedimentary tectonics and the resulting diverse platform architecture.

#### *Carbonate-Platform Response to the Late Cenomanian Sea Level Rise and OAE 2*

The CTB interval is associated globally with the sea-level rise and OAE 2 (Schlanger et al. 1987; Jarvis et al. 2006; among numerous others). Comparison with other strata regionally to globally indicated that the Adriatic carbonate platform was also affected by this important late Cenomanian–early Turonian event. The lithological differences across the Milna–Sveti Duh formation boundary include an increased component of planktonic faunal elements, indicative of a transgressive trend, and confirm that this part of the platform experienced sea-level rise in the late Cenomanian. As a result, the high abundance and diversity of large benthic organisms in the Milna Formation decreased abruptly at BBK (Fig. 2), and transitioned more gradually into primarily pelagic calcispheres in the overlying Sveti Duh Formation at BSV (Fig. 3). These and other lithological differences between BBK and BSV indicate different depositional settings for these two Brač successions (Figs. 2, 3). The presence of an interval of laminated deposits containing foraminifera indicative of brackish conditions (Fig. 5D) in the Milna Formation at BBK supports more restricted platform conditions at this locality (Fig. 8A, B). Laminated mudstones (Figs. 2, 4B, 5C) likely represent microbial laminites on a restricted shallow carbonate platform lagoon or intraplatform basin. In the Milna Formation of BBK, carbon-isotope values are about 2‰ lower than in the Milna Formation of BSV (Fig. 6). This may also reflect different depositional settings for these two successions; the Milna Formation laminites of BBK may be representative of a more restricted environment on the inner carbonate platform, and their  $\delta^{13}\text{C}$  values may reflect the local carbon-isotope signature of a setting with limited seawater circulation as compared to BSV (e.g., Immenhauser et al. 2008; and references therein). The sharp contact between the typical peritidal facies of the Milna Formation and the deeper-water predominantly muddy deposits of the Sveti Duh Formation in both studied sections indicates an environmental change from shallow, in places restricted carbonate platform to an open marine or drowned-platform setting (Fig. 8C).

Calcspheric wackestone–packstone in the matrix and intraclasts in the disturbed interval of the uppermost Milna Formation at BBK section indicate that sliding and slumping event(s) affected the BBK area after the deposition of the oldest drowned-platform sediments (Fig. 8D). These events resulted in mass sliding of the semilithified laminites and in breaking of other associated deposits into angular clasts, which were resedimented as intraformational carbonate breccia (Figs. 2, 4). The presence of neptunian dikes filled by calcspheric wackestone–packstone in the underlying shallow-platform deposits (Figs. 2, 5B), on the other hand, suggests the contemporaneous existence of an extensional regime. The extension probably initiated activation of the Milna fault and formation of a half-graben type intra-platform structure (Figs. 1D, 8C–



E). The Cenomanian extensional tectonics has been also reported elsewhere on the platform; extensional intraplateau basins are documented from the island of Cres (Korbar et al. 2001), while small-scale synsedimentary extensional features are reported from southern Istria (Tišljarić et al. 1998). This suggests that extensional tectonics was widespread in the region during the Cenomanian. Although beyond the scope of this paper, it should be also noted that south-verging slumps were formed during the late Cenomanian in both the northern (BBK section, Fig. 4B) and southern limbs (Prtoljan et al. 2007) of the present-day Milna anticline (Fig. 1D). This implies that the Cenozoic compressional tectonics which produced the Milna anticline was not simply inherited from the Cenomanian, but that the Late Cretaceous extensional tectonics was later overprinted during the Dinaridic (Alpine) compression (Korbar 2009).

Calcspheritic wackestone–packstone in sharp contact with the underlying disturbed interval referred to as the Milna Formation indicate that the open-platform deposition persisted after the local intraplateau mass transport. Late Cenomanian benthic foraminifera, which are rarely present as intercalations within the drowned-platform facies of the Sveti Duh Formation in the BBK succession (at 35.7 m; Figs. 2, 5F), suggest contemporaneous existence of shallow-platform environments relatively nearby or a temporary relative sea-level fall. This also suggests that biotic effects of the CTB perturbations, i.e., an obvious faunal turnover (Gušić and Jelaska 1990, 1993), did not happen during the early drowning of the platform, but was rather a consequence of multiple interrelated factors that influenced the environment during the CTB interval (e.g., Mitchell et al. 2008). Turonian index microfossils present in bioclastic intercalations from the uppermost part of the Sveti Duh Formation indicate platform recovery (Figs. 2, 3, 5).

Common intercalations of bioclastic packstone–rudstone in the upper part of the Sveti Duh Formation at BBK indicate that migration of major peritidal carbonate factories (including prograding banks) during the recovery of shallow-platform environments reached the BBK area prior to the BSV area (Fig. 8E). This resulted in an additional difference in thickness of the drowned-platform succession: the Sveti Duh Formation is thicker in the BSV section relative to the BBK. The documented variations in thickness of these drowned-platform successions can be explained by three superimposed mechanisms: (1) diachronous drowning of the platform relief; (2) intraplateau (local) redeposition(s) of parts of the successions by various mass-gravity transport processes, indicating enhanced instability due to increasing accommodation space related to the late Cenomanian platform drowning and intraplateau extensional tectonics; and (3) migration of major carbonate factories during the recovery of shallow-platform environments.

The absence of synsedimentary deformation features and the predominance of bioclastic deposits at BSV also suggest less restricted carbonate-platform conditions for the deposition of Milna Formation at BSV as opposed to BBK. In conjunction with the close proximity of the BSV and BBK sections (Fig. 8), this depicts and further supports the presence of diverse depositional environments in the region during the CTB time interval.

This study provides new information about the local to global correlation of strata from the Adriatic carbonate platform that was not previously possible due to the absence of high-resolution biostratigraphic and chemostratigraphic indicators. The results indicate that platform

drowning started at the first hint of the CTB positive carbon-isotope excursion event (peak “a”; Fig. 6), which is tentatively correlated with the beginning of the Plenus Cold Event (Jarvis et al. 2006; Pearce et al. 2009). This event is related to widespread deposition of black shale in basinal settings elsewhere (Schlanger et al. 1987), and probably coincides with the beginning of pelagic sedimentation over the carbonate platform in response to rapidly rising sea level during the late Cenomanian. The lack of black shale horizons in the studied platform-top successions suggests that the OAE 2 was a consequence of still debated synchronous processes (Mitchell et al. 2008) rather than an ultimate trigger of platform drowning. Widespread coeval organic-rich black shale deposits probably accumulated elsewhere in deeper (anoxic) settings below the rising sea level. On the other hand, the CTB interval event caused an unusual increase in accommodation space on the carbonate platform enabling open-marine influence and synsedimentary redeposition.

## CONCLUSIONS

- (1) The two analyzed carbonate rock successions from the Adriatic carbonate platform (*sensu stricto*) are characterized by a major lithological change at the boundary between the Milna and Sveti Duh formations. This change represents a shift from peritidal skeletal-rich facies and/or laminated microbial mudstone to pelagic carbonate deposits with abundant calcspheres in response to an environmental change from shallow, restricted carbonate platform to an open marine or drowned-platform setting.
- (2) The detailed biostratigraphic analyses confirm late Cenomanian age of the Milna Formation, late Cenomanian–early Turonian age of the Sveti Duh Formation, and Turonian age of the overlying Gornji Humac Formation.
- (3) Uniformly positive carbon isotope ( $\delta^{13}\text{C}$ ) values, averaging +3.5‰, are sustained over tens of meters of stratigraphic thickness in both analyzed successions and represent the Cenomanian–Turonian Boundary (CTB) interval excursion plateau. The  $\delta^{13}\text{C}$  values recover to the pre-excursion values of about +2‰ in the uppermost part of one succession (BSV), enabling a more precise placement of the CTB interval in the pelagic deposits of the Sveti Duh Formation. This boundary is stratigraphically higher than previously proposed, but without adequate biostratigraphic control, its exact position remains uncertain.
- (4) Carbon-isotope curves are correlated regionally and globally. Correlation with the reference section at Eastbourne (England) revealed that all three characteristic positive  $\delta^{13}\text{C}$  peaks (a, b, and c) of the CTB event can be tentatively recognized.
- (5) Documented variations in thickness of the drowned-platform successions can be explained by three superimposed mechanisms: (a) diachronous drowning of the platform relief; (b) intra-platform redeposition of parts of the successions by various mass-gravity transport processes (indicating enhanced instability due to increasing accommodation space related to the late Cenomanian platform drowning and synsedimentary tectonics); and (c) migration of major carbonate factories during the recovery of shallow-platform environments.
- (6) The documented positive carbon-isotope excursion corresponds to the global sea-level rise during the CTB perturbations and OAE

←

Fig. 8.—Interpretation of the late Cenomanian–early Turonian depositional dynamics in the studied carbonate platform area of the western part of the island of Brač (see maps in Fig. 1). Light gray = shallow-platform carbonates; Dark gray = drowned-platform carbonates. See text for further explanation of the depositional stages A–E (chronologically from the bottom to the top).

2. These penecontemporaneous processes caused a significant increase in accommodation space that allowed open-marine influence and syndimentary perturbations atop the platform. The coeval and widespread organic-rich black shale deposits reported from other regions probably accumulated in deeper (anoxic) setting below the rising sea level.

#### ACKNOWLEDGMENTS

This work was supported by the Croatian Ministry of Science, Education and Sports through the scientific project "Stratigraphy and Geodynamic Context of Cretaceous Deposits in the NE Adriatic Region" (No. 181-1191152-2697). BG was partially funded by Smith College. BCT and TK would like to thank Profs. V. Jelaska and I. Gušić (University of Zagreb, Croatia) for their continuous support and supervision of our earlier work. Technical staff of the Croatian Geological Survey helped with preparation of slabs and thin sections as well as with some figure drafts. Prof. S. Burns (University of Massachusetts, Amherst) is thanked for stable-isotope analyses. The paper benefited from highly constructive comments by Prof. A. Immenhauser (Ruhr-Universität Bochum, Germany), an anonymous reviewer, and JSR Editors E. Rankey and G. Ludvigson.

#### REFERENCES

- ARTHUR, M.A., SCHLANGER, S.O., AND JENKYN, H.C., 1987, The Cenomanian/Turonian Oceanic Anoxic Event, II: Paleocyanographic controls on organic matter production and preservation, *in* Brooks, J., and Fleet, A.J., eds., *Marine Petroleum Source Rocks*: Geological Society of London, Special Publication 26, p. 401–420.
- CHANNELL, J.E.T., D'ARGENIO, B., AND HORVATH, F., 1979, Adria, the African promontory, in Mesozoic Mediterranean palaeogeography: *Earth-Science Reviews*, v. 15, p. 213–292.
- DAVEY, S.D., AND JENKYN, H.C., 1999, Carbon-isotope stratigraphy of shallow-water limestones and implications for the timing of Late Cretaceous sea-level rise and anoxic events (Cenomanian–Turonian of the peri-Adriatic carbonate platform, Croatia): *Eclogae Geologicae Helveticae*, v. 92, p. 163–170.
- DERCOURT, J., GAETANI, M., VRIELYNCK, B., BARRIER, E., BIJU-DUVAL, B., BRUNET, M.F., CADET, J.P., CRASQUIN, S., AND SANDULESCU, M., eds., *Atlas Peri-Tethys, Palaeogeographical Maps: Commission for the Geological Map of the World*, Paris, 24 maps and explanatory notes, I–XX, 269 p.
- DESMARES, D., GROSHENY, D., BEAUDOIN, B., GARDIN, S., AND GAUTHIER-LAFAYE, F., 2007, High resolution stratigraphic record constrained by volcanic ash beds at the Cenomanian–Turonian boundary in the Western Interior Basin, USA: *Cretaceous Research*, v. 28, p. 561–582.
- FISHER, J.K., PRICE, G.D., HART, M.B., AND LENG, M.J., 2005, Stable isotope analysis of the Cenomanian–Turonian (Late Cretaceous) oceanic event in the Crimea: *Cretaceous Research*, v. 26, p. 853–863.
- GALE, A.S., KENNEDY, W.J., VOIGT, S., AND WALASZCZYK, I., 2005, Stratigraphy of the Upper Cenomanian–Lower Turonian Chalk succession at Eastbourne, Sussex, UK: ammonites, inoceramid bivalves and stable carbon isotopes: *Cretaceous Research*, v. 26, p. 460–487.
- GERTSCH, B., ADATTE, T., KELLER, G., TANTAWY, A.A.A.M., BERNER, Z., MORT, H.P., AND FLEITMANN, D., 2010, Middle and Late Cenomanian oceanic anoxic events in shallow and deeper shelf environments of western Morocco: *Sedimentology*, v. 57, p. 1430–1462.
- GROSHENY, D., BEAUDOIN, B., MOREL, L., AND DESMARES, D., 2006, High-resolution biostratigraphy and chemostratigraphy of the Cenomanian/Turonian boundary event in the Vocontian Basin, southeast France: *Cretaceous Research*, v. 27, p. 629–640.
- GUŠIĆ, I., AND JELASKA, V., 1990, Upper Cretaceous stratigraphy of the Island of Brač: *Djela Jugoslavenske akademije znanosti i umjetnosti Zagreb* 69, 160 p, 20 pls. [In Croatian with an extended English summary].
- GUŠIĆ, I., AND JELASKA, V., 1993, Upper Cenomanian–Lower Turonian sea-level rise and its consequences on the Adriatic–Dinaric carbonate platform: *Geologische Rundschau*, v. 82, p. 676–686.
- IMMENHAUSER, A., HOLMDEN, C., AND PATTERSON, W.P., 2008, Interpreting the carbon-isotope record of ancient shallow epeiric seas: lessons from the Recent, *in* Pratt, B.R., and Holmden, C., eds., *Dynamics of Epeiric Seas*: Geological Association of Canada, Special Paper 48, p. 137–174.
- JARVIS, I., GALE, A.S., JENKYN, H.C., AND PEARCE, M.A., 2006, Secular variation in Late Cretaceous carbon isotopes: a new  $\delta^{13}\text{C}$  carbonate reference curve for the Cenomanian–Campanian (99.6–70.6 Ma): *Geological Magazine*, v. 143, p. 561–608.
- JELASKA, V., 2002, Carbonate Platforms of the External Dinarides, *in* Vlahović, I., and Tišljarić, J., eds., *Evolution of Depositional Environments from the Palaeozoic to the Quaternary in the Karst Dinarides and Pannonian Basin*: 22nd International Association of Sedimentologists, Meeting of Sedimentology, Opatija, Field Trip Guidebook, p. 67–71.
- JENKYN, H.C., 1991, Impact of Cretaceous sea level rise and anoxic events on the Mesozoic carbonate platform of Yugoslavia: *American Association of Petroleum Geologists, Bulletin*, v. 75, p. 1007–1017.
- JENKYN, H.C., GALE, A.S., AND CORNFIELD, R.M., 1994, Carbon- and oxygen-isotope stratigraphy of the English Chalk and Italian Scaglia and its palaeoclimatic significance: *Geological Magazine*, v. 131, p. 1–34.
- KORBAR, T., 2009, Orogenic evolution of the External Dinarides in the NE Adriatic region: a model constrained by tectonostratigraphy of Upper Cretaceous to Paleogene carbonates: *Earth-Science Reviews*, v. 96, p. 296–312, doi: 10.1016/j.earscirev.2009.07.004.
- KORBAR, T., FUČEK, L., HUSINEC, A., VLAHOVIĆ, I., OŠTRIĆ, N., MATIČEC, D., AND JELASKA, V., 2001, Cenomanian carbonate facies and rudists along shallow intraplatform basin margin—the Island of Cres (Adriatic Sea, Croatia): *Facies*, v. 45, p. 39–58.
- KUMP, L.R., AND ARTHUR, M.A., 1999, Interpreting carbon-isotope excursions: carbonates and organic matter: *Chemical Geology*, v. 161, p. 181–198.
- MITCHELL, R.N., BICE, D.M., MONTANARI, A., CLEAVELAND, L.C., CHRISTIANSON, K.T., COCCIONI, R., AND HINNOV, L.A., 2008, Oceanic anoxic cycles? Orbital prelude to the Bonarelli Level (OAE 2): *Earth and Planetary Science Letters*, v. 267, p. 1–16.
- PALCI, A., JURKOVŠEK, B., KOLAR-JURKOVŠEK, T., AND CALDWELL, M.W., 2008, New palaeoenvironmental model for the Komen (Slovenia) Cenomanian (Upper Cretaceous) fossil *lagerstätte*: *Cretaceous Research*, v. 29, p. 316–328.
- PAMIĆ, J., GUŠIĆ, I., AND JELASKA, V., 1998, Geodynamic evolution of the Central Dinarides: *Tectonophysics*, v. 297, p. 251–268.
- PARENTE, M., FRUJA, G., AND DI LUCIA, M., 2007, Carbon-isotope stratigraphy of Cenomanian–Turonian platform carbonates from the southern Apennines (Italy): a chemostratigraphic approach to the problem of correlation between shallow-water and deep-water successions: *Geological Society of London Journal*, v. 164, p. 609–620.
- PAUL, C.R.C., LAMOLDA, M.A., MICHELL, S.F., VAZIRI, M.R., GOROSTIDI, A., AND MARSHALL, J.D., 1999, The Cenomanian–Turonian boundary at Eastbourne (Sussex, UK): a proposed European reference section: *Palaeogeography, Palaeoclimatology, Palaeoecology*, v. 150, p. 83–121.
- PEARCE, M.A., JARVIS, I., AND TOCHER, B.A., 2009, The Cenomanian–Turonian event, OAE2 and palaeoenvironmental change in epicontinental seas: New insights from the dinocyst and geochemical records: *Palaeogeography, Palaeoclimatology, Palaeoecology*, v. 280, p. 207–234.
- PRTOLIAN, B., JAMIČIĆ, D., CVETKO TEŠOVIĆ, B., KRATKOVIĆ, I., AND MARKULIN, Ž., 2007, The influence of Late Cretaceous syndimentary deformation on the Cenozoic structuration of the middle Adriatic, Croatia: *Geodinamica Acta*, v. 20, p. 287–300.
- SCHLANGER, S.O., ARTHUR, M.A., JENKYN, H.C., AND SCHOLLE, P.A., 1987, The Cenomanian–Turonian oceanic anoxic event, I. Stratigraphy and distribution of organic carbon-rich beds and the marine  $\delta^{13}\text{C}$  excursion, *in* Brooks, J., and Fleet, A.J., eds., *Marine Petroleum Source Rocks*: Geological Society of London, Special Publication 26, p. 371–400.
- STUEBER, T., KORBAR, T., JELASKA, V., AND GUŠIĆ, I., 2005, Strontium-isotope stratigraphy of Upper Cretaceous platform carbonates of the island of Brač (Adriatic Sea, Croatia): implications for global correlation of platform evolution and biostratigraphy: *Cretaceous Research*, v. 26, p. 741–756.
- SWART, P.K., REJMER, J.J.G., AND OTTO, R., 2009, Geochemical facies of Great Bahama Bank, *in* Swart, P.K., Eberli, G.P., and McKenzie, J., eds., *Perspective in Carbonate Geology: A Tribute to the Career of Robert Nathan Ginsburg*: International Association of Sedimentologists, Special Publication 41, p. 47–60.
- TIŠLIJAR, J., VLAHOVIĆ, I., VELIĆ, I., MATIČEC, D., AND ROBSON, J., 1998, Carbonate facies evolution from the Late Albian to Middle Cenomanian in southern Istria (Croatia): Influence of syndimentary tectonics and extensive organic carbonate production: *Facies*, v. 38, p. 137–152.
- VLAHOVIĆ, I., TIŠLIJAR, J., VELIĆ, I., AND MATIČEC, D., 2005, Evolution of the Adriatic Carbonate Platform: palaeogeography, main events and depositional dynamics: *Palaeogeography, Palaeoclimatology, Palaeoecology*, v. 220, p. 333–360.
- WEISSERT, H., 1989, C-isotope stratigraphy, a monitor of paleoenvironmental change: a case study from the Early Cretaceous: *Surveys in Geophysics*, v. 10, p. 1–61.
- ZAPPATERA, E., 1994, Source rock distribution model of the Periadriatic region: *American Association of Petroleum Geologists, Bulletin*, v. 78, p. 333–354.

Received 20 September 2010; accepted 22 October 2011.